

## Integrated mass spectrometry reveals celastrol as a novel catechol-O-methyltransferase inhibitor

Haijun Guo <sup>a†</sup>, Yang Yang <sup>a†</sup>, Qi Zhang <sup>a,b†</sup>, Jie-Ren Deng <sup>a</sup>, Ying Yang <sup>a</sup>, Shuqi Li <sup>a</sup>, Pui-Kin So <sup>e</sup>,  
Thomas C. Lam <sup>b,c,d</sup>, Man-kin Wong <sup>a</sup>, Qian Zhao <sup>\*a</sup>

a. State Key Laboratory of Chemical Biology and Drug Discovery, Department of Applied Biology and Chemical Technology, The Hong Kong Polytechnic University, Hong Kong, SAR 999077, China

b. Centre for Eye and Vision Research, 17W Hong Kong Science Park, Hong Kong, SAR 999077, China

c. Centre for Myopia Research, School of Optometry, The Hong Kong Polytechnic University, Hong Kong, SAR 999077, China

d. Research Centre for SHARP Vision, The Hong Kong Polytechnic University, Hong Kong, SAR 999077, China

e. University Research Facility in Life Sciences, The Hong Kong Polytechnic University, Hong Kong, SAR 999077, China

\*Corresponding Author, Email: [q.zhao@polyu.edu.hk](mailto:q.zhao@polyu.edu.hk)

† The authors contributed equally

## ABSTRACT

Natural product celastrol is known to have various biological activities, yet its molecular targets that correspond to many activities remain unclear. Here we used multiple mass spectrometry-based approaches to identify catechol-O-methyltransferase (COMT) as a major binding target of celastrol and characterized their interaction comprehensively. Celastrol was found to inhibit the enzymatic activity of COMT and increased dopamine level in neuroendocrine chromaffin cells significantly. Our study not only revealed a novel binding target of celastrol, but also provided a new scaffold and cysteine hot spot for developing new generation COMT inhibitors in combating neurological disorders.

## INTRODUCTION

Natural products have been a treasure trove for drug discovery. From 1940 to 2020, 66.7% of the approved small-molecule drugs are either natural products or their derivatives.<sup>1</sup> How to get a comprehensive understanding of the mode of actions of natural products is one of the major challenges when developing them into drugs. Therefore, it is essential to identify the direct binding partners and precise sites of natural products for resolving their mechanisms.

Celastrol, a pentacyclic triterpene with electrophilic quinone methide extracted from *Tripterygium wilfordii*, was recognized as one of five promising natural products for drug discovery.<sup>2</sup> In the past decades, extensive studies have revealed its broad spectrum of activities in anti-obesity, anticancer, anti-inflammation and neuroprotection.<sup>3-5</sup> Although considerable efforts have been made to reveal multiple binding targets,<sup>6-9</sup> many biological activities of celastrol cannot be explained with the known targets. For example, in a preclinical testing for neurodegenerative diseases, celastrol was found to confer potent dopaminergic neuroprotection in *Drosophila* Parkinson's disease model.<sup>10</sup> However, the mechanism through which celastrol increased dopamine level in the brain was unknown, thus the search for targets with high functional significance is called for.

COMT is a methyltransferase that metabolizes catechol estrogens and catechol neurotransmitters such as dopamine (DA). In clinical practice, COMT inhibitors are used in combination with levodopa, the precursor of dopamine, to control the motor symptoms of Parkinson's disease. COMT inhibitors have also been proposed to treat other diseases such as Alzheimer's disease, schizophrenia and deficit hyperactivity disorder, etc.<sup>11-13</sup> Unfortunately, further applications of currently available COMT inhibitors have been limited by their insufficient brain penetration or severe side effect.<sup>14, 15</sup>

Here, we applied chemical proteomics to identify COMT as a major binding target of celastrol and verified the finding with targeted mass spectrometry methods. We also analyzed the binding stoichiometry between celastrol and COMT with time-of-flight mass spectrometry. Celastrol covalently attached to COMT and inhibited the enzymatic activity of both soluble isoform S-COMT and membrane-bound form MB-COMT, and thus induced a significant increase of DA in neuroendocrine chromaffin cells. We found that celastrol inhibited enzymatic activity mainly through targeting a cysteine residue, which is a new mechanism to inhibit COMT.

## RESULT AND DISCUSSION

First, we sought to develop a “clickable” probe, which retained the bioactivity of celastrol and bound to celastrol’s cellular targets in live cells. Based on the reported structure-activity relationship,<sup>16</sup> we synthesized four probes by derivatizing the carboxyl terminus of celastrol with terminal alkyne groups via various linkers (Figure 1A and Figure S1). Celastrol was known to suppress inflammation through inhibiting NF- $\kappa$ B pathway, with I $\kappa$ B $\alpha$  degradation as a hallmark.<sup>17</sup> With the assay, all four probes were shown to inhibit PMA-induced I $\kappa$ B $\alpha$  degradation, demonstrating their anti-inflammatory activities (Figure S2). In another assay when compounds were used to suppress tumor cell viability, the half maximal inhibitory concentrations (IC<sub>50</sub>) of probes to inhibit Jurkat cell growth ranged from 1.17  $\mu$ M to 3.11  $\mu$ M, which were comparable to that of celastrol (9.51  $\mu$ M) (Figure S3).

Next, the labeling efficiency and specificity of the four probes for the target proteins were compared side by side. Live Jurkat cells were treated with vehicle or excess celastrol followed by labeling with respective probes. In the in-gel fluorescence scan, C1a showed the strongest intensity. Many proteins labeled by C1a were competed away by celastrol, which demonstrated the labeling specificity of C1a (Figure S4). As a considerable background was seen in probe-labeled Jurkat cells, we compared three cell lines. HeLa S3 cells displayed the lowest background with an outstanding protein band strongly labeled at around 30 kDa (Figure 1B). Remarkably, probe labeling of this protein band was almost completely abolished by celastrol in all three cell types, suggesting the high specificity and high affinity of the interaction between celastrol and this protein (pointed by red arrow). Therefore, we chose C1a probe and HeLa S3 cells to perform the subsequent target identification experiments.

Then, we performed target profiling of celastrol with stable isotope labeling with amino acids in cell culture (SILAC). In forward SILAC, heavy isotope-labeled cells (Heavy, H) were treated with

C1a, and regular cells (Light, L) were treated with celastrol followed by C1a. In a reciprocal experiment, the treatment was swapped in the reverse SILAC. As illustrated in Figure S5, cell lysate was harvested after treatment and conjugated to biotin-azide via click reaction. The probe-labeled proteins were enriched with streptavidin magnetic beads, then digested and subjected to liquid chromatography with tandem mass spectrometry (LC-MS/MS) analysis. Among hundreds of proteins that were detected by MS, COMT was found to be among the significantly highly enriched ones that of MS intensity over 1E8 (Figure S6A). Meanwhile, the intensity of COMT dropped by over 10-fold in the presence of celastrol competition, indicating a strong interaction with the parent compound celastrol. Such observation was consistent in both forward and reserve SILAC experiments (Figure 1C and Table S1). We also performed three target identification experiments independently by using label-free quantitative (LFQ) proteomics. We found known targets of celastrol including IKKB<sup>17</sup> (Figure 1C), as well as some potential new targets. Although the enrichment methods in three LFQ target identification experiments were different, COMT was consistently identified among the top-ranked candidates and was the only one with highly reproducibility (Figure S6B, C and Table S2).

Next, we validated COMT as a potential target identified in chemical proteomics with multiple independent assays. First, we re-analyzed the pulldown products with targeted mass spectrometry approach, namely parallel reaction monitoring (PRM). The ions of two COMT peptides with unique sequences (<sup>152</sup>MVDFAGVK<sup>159</sup> and <sup>252</sup>EVVDGLEK<sup>259</sup>) were selected and accurately quantified. Despite their differential MS responses and intensities, both peptides were enriched by C1a and inhibited by 10-fold celastrol (Figure 2A). Mammalian COMT gene encodes both a full-length MB-COMT and soluble isoform S-COMT. Both COMTs catalyze the regioselective transfer of a methyl group from S-Adenosyl Methionine (SAM) to one hydroxyl group of its catechol substrates such as dopamine.<sup>18</sup> S-COMT is mainly located in cytosolic fraction of periphery, and MB-COMT is considered to be more important in the central nervous system.<sup>19</sup> To differentiate between the interaction of celastrol with S-COMT and MB-COMT, we knocked down the expression of endogenous COMTs in HeLa S3 cells and observed the change in fluorescence signal as a result of C1a labeling. Both expressions of MB-COMT and S-COMT decreased, which led to a decrease in fluorescent intensity after probe labeling (Figure 2B). Meanwhile, a chemical precipitation assay was performed by detecting COMT in pulldown products with anti-COMT antibody (Figure S7). It was noteworthy that although the endogenous S-COMT was detectable in western blot, the probe labeling

of C1a in S-COMT was barely seen, much weaker than that of MB-COMT. This observation was consistent with that in Figure S7, where S-COMT was barely detectable in the proteins enriched with C1a. We also overexpressed MB-COMT in HEK293T cells, which in turn resulted an additional protein band with strong fluorescence signal, demonstrating effective labeling by C1a (Figure 2C). Therefore, we reasoned that celastrol preferentially bound to MB-COMT over S-COMT in live cells. To visualize the celastrol-COMT interaction and their engagement with each other in cells, we also performed fluorescent staining with HeLa cells. Under confocal microscope, COMT was labeled as green fluorescence after immunostaining with anti-COMT antibody. C1a-labeled proteins were labeled as red after click with tetramethylrhodamine (TAMRA)-azide. The overlay of green from endogenous COMT and red from C1a demonstrated co-localization of celastrol with COMT in cells (Figure 2D, S8). According to previous report<sup>20</sup>, MB-COMT is not only located in plasma membrane, but also in endoplasmic reticulum (ER). Consistently, here we observed fluorescent signal from C1a labeling co-localized with COMT in ER.

Key cysteines were reported as useful hot spots for irreversible inhibitors to attack.<sup>21, 22</sup> Celastrol was also reported to covalently react with thiol-containing agents, via Michael addition. We reasoned that the cysteine sidechain of COMT reacts with celastrol via a nucleophilic Michael addition at celastrol's C6 position (Figure S9A). To this end, wild type (WT) S-COMT, WT MB-COMT and mutated S-COMT were purified to evaluate their interactions with celastrol (Table S3). Recombinant proteins were incubated with celastrol at various concentrations followed by C1a labeling and click reaction. In this competitive experiment, a decrease in fluorescence signal in the protein bands indicated interaction with celastrol. It was observed that the apparent  $IC_{50}$  values of celastrol in S-COMT and MB-COMT were close under the in-vitro conditions (Figure S10). Because MB-COMT was strongly labeled and visualized as fluorescence in live cell images, we could quantify the  $IC_{50}$  of celastrol in MB-COMT in live cells as well. The in-situ  $IC_{50}$  of celastrol in MB-COMT was almost 20 times lower than the in-vitro  $IC_{50}$ , suggesting high affinity between celastrol and MB-COMT in live cells. However, given that S-COMT showed better solubility and was easier produced, all the following mutagenesis and enzymatic assays were carried out with S-COMT.

Next, we adopted an alternative approach by reading celastrol's UV absorption at 440 nm to monitor the interactions. After WT S-COMT or mutants were incubated with celastrol, the absorption of free celastrol was significantly decreased, indicating new bond formation during interaction

(Figure 3A, S9A). To further investigate whether the covalent bond was reversible or irreversible, we diluted the celastrol-S-COMT adduct, or celastrol alone in PBS. As a comparison, the reversible adduct formed by celastrol and  $\beta$ -Mercaptoethanol ( $\beta$ -ME) was diluted with PBS. Consistent with previous report<sup>23</sup>, the reversible adduct formed by  $\beta$ -ME and celastrol decomposed when it was diluted in PBS because the equilibrium of reaction was reversed due to dilution of reactant ( $\beta$ -ME). As expected, the adduct remained stable when it was diluted in  $\beta$ -ME. In contrast, the UV absorption, an indicator of celastrol-COMT adduct formation, did not change no matter if the celastrol-COMT adduct was diluted in PBS or excess celastrol, demonstrating that the covalent bound between celastrol and COMT was irreversible under the tested conditions (Figure S11). In this sense, COMT is different from other reported celastrol's targets.<sup>23</sup> To further pin down the exact binding sites, we mutated five cysteines (C) that are exposed on the surface of S-COMT into alanine (A) to get C95A, C157A, C173A, C188A and C191A (Figure S9B, C). Compared with WT S-COMT, mutants of C157A and C95A showed weaker abilities to reduce the UV absorption of celastrol, suggesting that C157 and C95 are very likely to interact with celastrol (Figure 3A). In agreement with the observation in UV absorption assay, C95A and C157A showed weaker interaction with C1a in an in-gel fluorescence scan (Figure 3B). Notably, C157A showed the most significant decrease in fluorescence signal among all mutants, suggesting C157 was the primary binding residue of celastrol.

To evaluate the binding stoichiometry of celastrol in COMT, we further performed ESI-Q-TOF MS analysis on intact recombinant S-COMT and mutants pretreated with celastrol. After treatment with celastrol at 4 °C for 2 hours, new peaks appeared with a mass shift of 450.4, 901.1 and 1351.8 Da, corresponding to conjugation of one, two and three celastrol molecules, respectively. Next, we performed the same analysis with five S-COMT mutants: C95A, C157A, C188A, C173A and C191A. Consistent with the two prior experiments (Figure 3A, B), both C173A and C191A COMT still bound to celastrol molecules (Figure S12). For C95A and C188A, the species bound with one or two celastrol molecules decreased dramatically while the species bound with three celastrol vanished. Remarkably, all interactions between celastrol and COMT were completely disrupted when a single residue C157 was mutated, again demonstrating this residue should be the key binding site (Figure 3C, S12). Besides, we performed tandem MS analysis to show direct binding sites of celastrol with purified COMT proteins. COMT was incubated with 7-fold celastrol followed by trypsin digestion

and LC-MS/MS analysis. The MS spectra confirmed that celastrol directly bound to C157 of COMT (Figure S13).

All celastrol-COMT complexes were robust to the strong acid condition during intact protein MS analysis, which again suggested that celastrol covalently bound to the cysteine residues irreversibly. COMT is an important methyltransferase, therefore we wondered whether celastrol had any impact on its enzymatic activity. As COMT catalyzes the methyl transfer from SAM to 3,4-Dihydroxyacetophenone (DHAP), its enzymatic activity can be monitored based on the absorption of DHAP at 340 nm.<sup>24</sup> In our results, COMT's enzymatic activity was inhibited by celastrol in a dose-response manner. MB-COMT showed slightly higher sensitivity to celastrol treatment, with an IC<sub>50</sub> of 3.81±0.34 μM, compared with that of S-COMT (6.22±0.34 μM) (Figure 4A). In a time-dependent experiment, the observed half-effective time of celastrol to inhibit S-COMT and MB-COMT were 15.6 and 12.6 minutes, respectively (Figure 4B). Furthermore, mutations of C173, C188 and C191 did not influence the inhibition of COMT enzymatic activity by celastrol, while mutation of C157 suppressed the inhibitory ability of celastrol significantly, indicating that celastrol inhibited enzymatic activities of COMTs through mainly targeting C157 (Figure S14). Human COMT is known to inactivate catechol hormones such as DA and catecholamine neurotransmitters by transferring methyl groups from the SAM to DA, which in turn generates 3-methoxytyramine (3-MT). A significant increase of DA as well as a significant decrease of 3-MT were observed upon celastrol treatment in a dose-dependent manner (Figure 4C, D). Treatment of 1 μM celastrol resulted in 6-fold increase of DA. Considering that celastrol did not affect the expression or stability of COMT in PC-12 cell (Figure S15), it was plausible that the change of DA and its metabolite catalyzed by COMT attributed to the inhibition of COMT enzymatic activity.

In conclusion, we have synthesized chemical probes to mimic the natural product celastrol and identified COMT as its major binding target with comprehensive chemical proteomics approaches. The covalent irreversible interaction between celastrol and COMT was validated with independent assays including targeted mass spectrometry and immunostaining. Celastrol bound to both S-COMT and MB-COMT and inhibited the enzymatic activities of both isoforms. C157 of S-COMT was found to be the primary binding site of celastrol. The conversion of DA to its downstream metabolite 3-MT, a process catalyzed by COMT, was inhibited by celastrol in neuroendocrine chromaffin cells. So far, clinically relevant COMT inhibitors are tight-binding nitrocatechols, which suffer from either a high

risk of liver damage and limited brain penetration.<sup>25</sup> Unlike the first-generation or second-generation COMT inhibitors,<sup>26,27</sup> celastrol can inhibit COMT enzymatic activity by binding to C157 which is at one terminal of the  $\alpha$ -helix (D141-C157, cyan area in Figure S9) that bridges SAM-binding pocket and substrate-binding pocket. Considering that the enzymatic activity might be vulnerable to seemingly minor structural perturbations around critical residue even far from the active pocket, it is possible for celastrol to disrupt COMT activity through inducing structural change of the  $\alpha$ -helix. Another similar unexpected inactivation was previously observed in the mutant V108M,<sup>28</sup> where local structure of COMT catalytic site was mildly perturbed, leading to decreased stability and reduced enzymatic activity. We discovered that C157 was also a key residue for celastrol to regulate COMT enzymatic activity. This residue can potentially serve as a targetable hot spot for developing inhibitors with mechanisms that are completely different from existing ones.

In brief, our study not only identified a new target of celastrol that expanded our knowledge on the mechanisms of celastrol, but also provided a novel scaffold and strategy for developing the next generation COMT inhibitors with great potential to tackle neurological disorders. Three complementary mass spectrometry approaches enabled us to decipher the interactions, which collectively demonstrated the power of analytical chemistry in solving fundamental biology questions.

*Supporting Information Available:* Experimental details and supplementary figures and tables including NMR spectra of chemical probe, in-gel and immunofluorescence analysis, illustration of COMT-celastrol interaction, enzymatic activity assay, MS-identified protein list, primer sequences for COMT mutant establishment and so on can be found in the Supporting Information.

## ACKNOWLEDGEMENTS

We acknowledge the funding support from Research Grants Council-ECS 25301518, GRF 15304819, CRF C5033-19E, and RGC-RIF R5050-18, NSFC 21705136. We thank the support from Centre for Eye and Vision Research (CEVR) and Laboratory for Synthetic Chemistry and Chemical Biology Limited (LSCCB) under the Health@InnoHK Programme launched by ITC, HKSAR. We thank Research Institute for Future Food (RiFood), the PolyU Research Facilities UCEA and ULS, C. Tsang, for technical support.

## CONFLICTS OF INTEREST

There are no conflicts to declare.

## REFERENCES

1. Newman, D. J., Cragg, G. M. (2020) Natural products as sources of new drugs over the nearly four decades from 01/1981 to 09/2019. *J. Nat. Prod.* 83 (3), 770-803.
2. Corson, T. W., Crews, C. M. (2007) Molecular understanding and modern application of traditional medicines: triumphs and trials. *Cell* 130 (5), 769-774.
3. Liu, J., Lee, J., Salazar Hernandez, M. A., Mazitschek, R., Ozcan, U. (2015) Treatment of obesity with celastrol. *Cell* 161 (5), 999-1011.
4. Wu, J., Hong, C., Pan, H., Yang, Q., Mei, Y., Ping Dou, Q., Yang, H. (2016) Medicinal Compound Celastrol As a Potential Clinical Anticancer Drug: Lessons Learned From Preclinical Studies. *Clin. Cancer Drugs* 3 (1), 63-73.
5. Zhang, B., Zhong, Q., Chen, X., Wu, X., Sha, R., Song, G., Zhang, C.; Chen, X. (2020) Neuroprotective effects of celastrol on transient global cerebral ischemia rats via regulating HMGB1/NF- $\kappa$ B signaling pathway. *Front. Neurosci.* 14, 847.
6. Chen, X., Zhao, Y., Luo, W., Chen, S., Lin, F., Zhang, X., Fan, S., Shen, X., Wang, Y., Liang, G. (2020) Celastrol induces ROS-mediated apoptosis via directly targeting peroxiredoxin-2 in gastric cancer cells. *Theranostics* 10 (22), 10290.
7. Kyriakou, E., Schmidt, S., Dodd, G. T., Pfuhlmann, K., Simonds, S. E., Lenhart, D., Geerlof, A., Schriever, S. C., De Angelis, M., Schramm, K.-W. (2018) Celastrol promotes weight loss in diet-induced obesity by inhibiting the protein tyrosine phosphatases PTP1B and TCPTP in the hypothalamus. *J. Med. Chem.* 61 (24), 11144-11157.
8. Ye, S., Luo, W., Khan, Z. A., Wu, G., Xuan, L., Shan, P., Lin, K., Chen, T., Wang, J., Hu, X. (2020) Celastrol attenuates angiotensin II-induced cardiac remodeling by targeting STAT3. *Circ. Res.* 126 (8), 1007-1023.
9. Liu, D., Luo, P., Gu, L., Zhang, Q., Gao, P., Zhu, Y., Chen, X., Zhang, J., Ma, N., Wang, J. (2021) Celastrol Exerts Neuroprotective Effect via Directly Binding to Hmgb1 Protein in Cerebral Ischemic Reperfusion. *J. Neuroinflammation* 18, 174.

10. Faust, K., Gehrke, S., Yang, Y., Yang, L., Beal, M. F., Lu, B. (2009) Neuroprotective effects of compounds with antioxidant and anti-inflammatory properties in a *Drosophila* model of Parkinson's disease. *BMC Neurosci.* 10 (1), 1-17.
11. Sweet, R., Devlin, B., Pollock, B., Sukonick, D., Kastango, K., Bacanu, S., Chowdari, K., DeKosky, S., Ferrell, R. (2005) Catechol-O-methyltransferase haplotypes are associated with psychosis in Alzheimer disease. *Mol. Psychiatry* 10 (11), 1026-1036.
12. Egan, M. F., Goldberg, T. E., Kolachana, B. S., Callicott, J. H., Mazzanti, C. M., Straub, R. E., Goldman, D., Weinberger, D. R. (2001) Effect of COMT Val108/158 Met genotype on frontal lobe function and risk for schizophrenia. *Proc. Natl Acad. Sci. U.S.A.* 98 (12), 6917-6922.
13. Paloyelis, Y., Asherson, P., Mehta, M. A., Faraone, S. V., Kuntsi, J. (2010) DAT1 and COMT effects on delay discounting and trait impulsivity in male adolescents with attention deficit/hyperactivity disorder and healthy controls. *Neuropsychopharmacology* 35 (12), 2414-2426.
14. Xia, Y., Pang, H., Dou, T., Wang, P., Ge, G. (2018) Interspecies comparison in the COMT-mediated methylation of 3-BTD. *RSC Adv.* 8 (29), 16278-16284.
15. Silva, T. B., Borges, F., Serrão, M. P., Soares-da-Silva, P. (2020) Liver says no: the ongoing search for safe catechol O-methyltransferase inhibitors to replace tolcapone. *Drug Discov. Today* 25 (10), 1846-1854.
16. Hou, W., Liu, B., Xu, H. (2020) Celastrol: Progresses in structure-modifications, structure-activity relationships, pharmacology and toxicology. *Eur. J. Med. Chem.* 189, 112081.
17. Lee, J.-H., Koo, T. H., Yoon, H., Jung, H. S., Jin, H. Z., Lee, K., Hong, Y.-S., Lee, J. J. (2006) Inhibition of NF- $\kappa$ B activation through targeting I $\kappa$ B kinase by celastrol, a quinone methide triterpenoid. *Biochem. Pharmacol.* 72 (10), 1311-1321.
18. Buchler, I., Akuma, D., Au, V., Carr, G., De León, P., DePasquale, M., Ernst, G., Huang, Y., Kimos, M., Kolobova, A. (2018) Optimization of 8-hydroxyquinolines as inhibitors of catechol O-methyltransferase. *J. Med. Chem.* 61 (21), 9647-9665.
19. Su, Y., DePasquale, M., Liao, G., Buchler, I., Zhang, G., Byers, S., Carr, G. V., Barrow, J., Wei, H. (2021) Membrane bound catechol-O-methyltransferase is the dominant isoform for dopamine metabolism in PC12 cells and rat brain. *Eur. J. Pharmacol.* 896, 173909.
20. Myöhänen, T.T., Männistö, P.T. (2010) Distribution and functions of catechol-O-methyltransferase proteins: do recent findings change the picture? *Int. Rev. Neurobiol.* 95, 29-47.

21. Liu, Q., Sabnis, Y., Zhao, Z., Zhang, T., Buhrlage, S. J., Jones, L. H., Gray, N. S. (2013) Developing irreversible inhibitors of the protein kinase cysteinome. *Chem. Biol.* 20 (2), 146-159.
22. Zhang, Y., Qin, W., Liu, D., Liu, Y., Wang, C. (2021) Chemoproteomic profiling of itaconations in Salmonella. *Chem. Sci.* 12 (17), 6059-6063.
23. Zhou, Y., Li, W., Wang, M., Zhang, X., Zhang, H., Tong, X., Xiao, Y. (2017) Competitive profiling of celastrol targets in human cervical cancer HeLa cells via quantitative chemical proteomics. *Mol. Biosyst.* 13 (1), 83-91.
24. Bartl, J., Palazzesi, F., Parrinello, M., Hommers, L., Riederer, P., Walitza, S., Grünblatt, E. (2017) The impact of methylphenidate and its enantiomers on dopamine synthesis and metabolism in vitro. *Prog. Psychopharmacol. Biol. Psychiatry* 79, 281-288.
25. Waters, C. (2000) Catechol-O-Methyltransferase (COMT) Inhibitors in Parkinson's Disease. *J. Am. Geriatr. Soc.* 48 (6), 692-698.
26. Lautala, P., Ulmanen, I., Taskinen, J. (2001) Molecular mechanisms controlling the rate and specificity of catechol O-methylation by human soluble catechol O-methyltransferase. *Mol. Pharmacol.* 59 (2), 393-402.
27. Kiss, L. s. E., Soares-da-Silva, P. (2014) Medicinal chemistry of catechol O-methyltransferase (COMT) inhibitors and their therapeutic utility. *J. Med. Chem.* 57 (21), 8692-8717.
28. Li, Y., Yang, X., Chang, M., Yager, J. D., Van Breemen, R. B., Bolton, J. L. (2005) Functional and structural comparisons of cysteine residues in the Val108 wild type and Met108 variant of human soluble catechol O-methyltransferase. *Chemico-biological interactions* 152 (2-3), 151-163.

## Figures and Legends

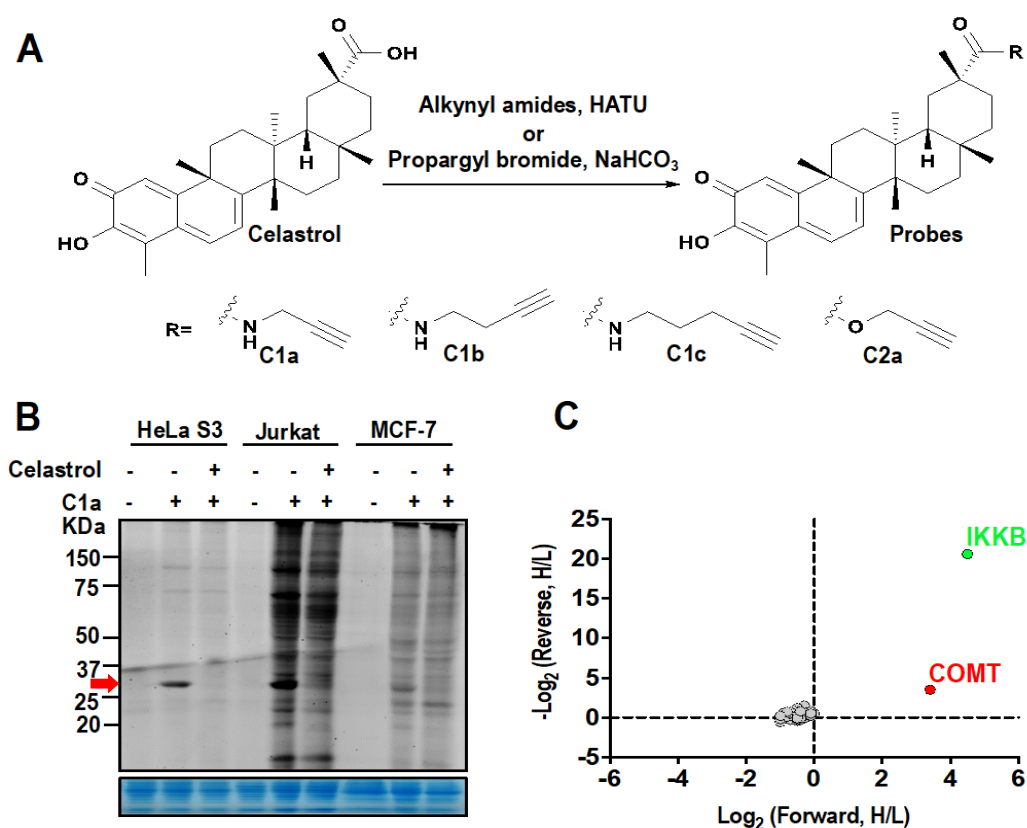


**Figure 1** Celastrol-based chemical probes for target identification. (A) Chemical structures and simplified synthesis routes of chemical probes. (B) In-gel fluorescence scan of proteins labeled by 2  $\mu$ M C1a probe after 10-fold celastrol treatment in different cell lines. Red arrow indicates the potential target specifically labeled by C1a. (C) A two-dimensional plot showing the  $\text{Log}_2$  values of SILAC ratios of each identified protein. Forward: heavy cells treated with 2  $\mu$ M C1a probe, light cells treated with 20  $\mu$ M celastrol followed by C1a probe. Reverse: light cells treated with C1a probe, heavy cells treated with celastrol followed by C1a probe. First, identified proteins were exported for CRAPome filtering with a cut-off frequency of 0.2. Then, probe-enriched proteins with MS intensity over  $1\text{E}8$  were selected for target screening. N.A. values of protein intensities were replaced by '100' to calculate SILAC ratios.

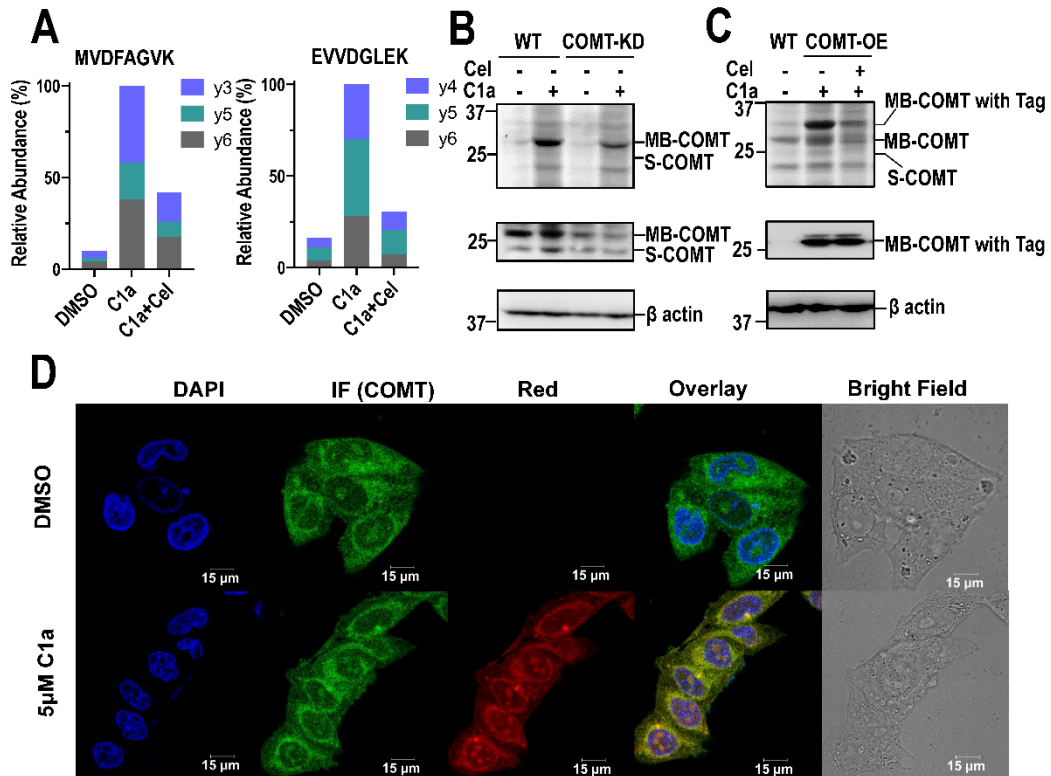


**Figure 2** Validation of the covalent interaction between COMT and celastrol. (A) Targeted MS analysis of two unique peptides of COMT. Cells were treated with 20 µM celastrol followed by 2 µM C1a probe. (B-C) Fluorescence labeling of COMT knockdown (KD) in HeLa S3 cells (B) and COMT overexpression (OE) in HEK293T cells (C) after living cells were treated with celastrol or C1a. (D) Immunofluorescence analysis showing the distribution of endogenous COMT and celastrol in HeLa cells. Blue channel: DAPI. Green channel: COMT. Red channel: C1a. Yellow channel: Overlap of COMT and C1a.

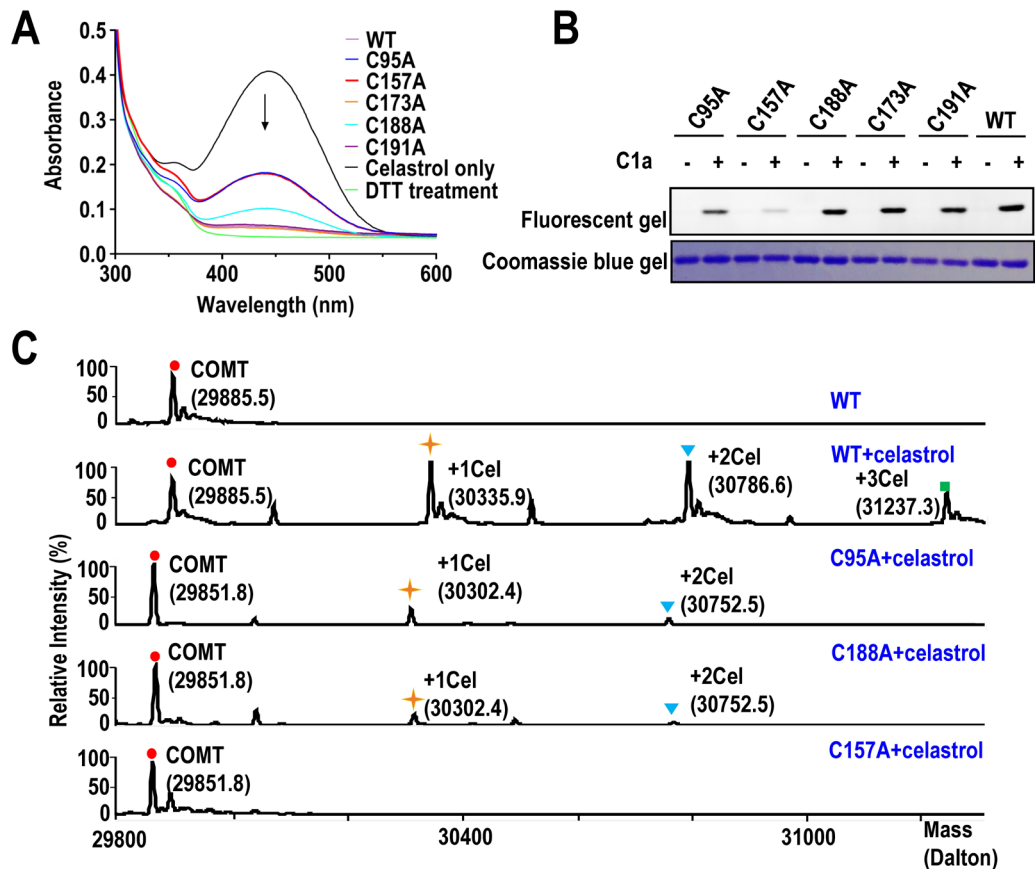


**Figure 3** Characterization of celastrol binding site on COMT. (A) UV absorption by 50  $\mu$ M celastrol at 440 nm after incubation with indicated with 0.25 eq. recombinant proteins at room temperature. (B) Labeling 1.67  $\mu$ M recombinant COMT or mutants with or without 12  $\mu$ M C1a at 4  $^{\circ}$ C overnight, followed by click reaction and in-gel fluorescence scanning. (C) MS analysis of wildtype or mutant COMT in complex with celastrol at 4  $^{\circ}$ C for 2 h.

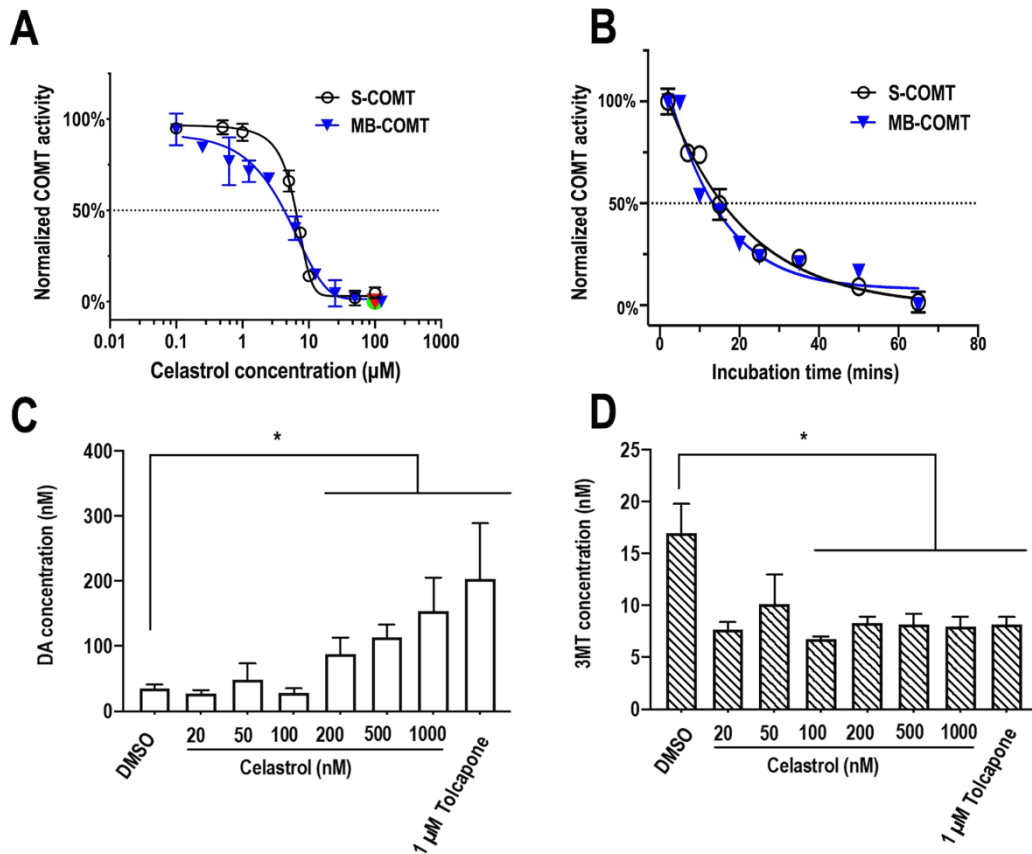


**Figure 4** The effect of celastrol on enzymatic activity of COMT *in vitro* and *in situ*. Purified S-COMT and MB-COMT were treated with celastrol at indicated concentrations before they catalyzed the methyl transfer from SAM to DHAP. (A) The enzymatic activities of 0.7 μM S-COMT and MB-COMT after incubation with celastrol at indicated concentrations at room temperature for 1 hour, the red triangles and green circle indicated the inhibition by 100 μM entacapone on MB-COMT and S-COMT, respectively. (B) The reaction kinetics after 0.7 μM S-COMT and MB-COMT were incubated with 50 μM celastrol at indicated time point at room temperature. Half maximal inhibitory concentration ( $IC_{50}$ ) and half-inhibition time ( $t_{1/2}$ ) were calculated. (C-D) Measurement of DA and 3-MT in PC-12 cells by using mass spectrometry after treatment of celastrol and tolcapone under 37°C/5%  $CO_2$ , \* $p < 0.05$ .

**For Table of Contents Only**

